Current Medical Science
DOI https://doi.org/10.1007/s11596-022-2621-5
42(6):1310-1318,2022

Gadolinium Enhances Dual-energy Computed Tomography Scan of Pulmonary Artery*

An XIE[1†], Wen-jie SUN[1†], Yan-feng ZENG[2], Peng LIU[1], Jian-bin LIU[1#], Feng HUANG[1#]
[1]*Department of Radiology, Hunan Provincial People's Hospital, First Affiliated Hospital of Hunan Normal University, Changsha 410005, China*
[2]*Department of Radiology, Hunan Chest Hospital, Changsha 410013, China*

[Abstract] Objective: To evaluate the feasibility of using gadopentetate dimeglumine (Gd-DTPA) for dual-energy computed tomography pulmonary angiography (CTPA). **Methods:** Sixty-six patients were randomly divided into three groups and underwent CTPA. Group A had a turbo flash scan using an iohexol injection, Group B had a turbo flash scan using Gd-DTPA, and Group C had a dual-energy scan using Gd-DTPA. The original images of Group C were linearly blended with a blending factor of 0.5 or reconstructed at 40, 50, 60, 70, 80, 90, 100, and 110 keV, respectively. The groups were compared in terms of pulmonary artery CT value, image quality, and radiation dose. **Results:** The pulmonary artery CT values were significantly higher in Group $C_{40\ \mathrm{keV}}$ than in Groups B and C, but lower than in Group A. There was no significant difference in the image noise of Groups $C_{40\ \mathrm{keV}}$, B, and C. Moreover, Group A had the largest beam hardening artifacts of the superior vena cava (SVC), followed by Groups B and C. Group $C_{40\ \mathrm{keV}}$ showed better vascular branching than the other three groups, among which Group B was superior to Group A. The subjective score of the image quality of Groups A, B, and C showed no significant difference, but the score was significantly higher in Group $C_{40\ \mathrm{keV}}$ than in Groups A and B. The radiation dose was significantly lower in Group B than in Groups A and C. **Conclusion:** Gd-CTPA is recommended to patients who are unsuitable for receiving an iodine-based CTPA. Furthermore, a turbo flash scan could surpass a dual-energy scan without consideration for virtual monoenergetic imaging.
Key words: gadopentetate dimeglumine; computed tomography pulmonary angiography; dual-energy scan; turbo flash scan; virtual monoenergetic imaging

A pulmonary embolism (PE), which refers to a blood clot that obstructs pulmonary circulation, is the third most common cause of cardiovascular deaths worldwide[1]. The short-term prognosis of a PE can be significantly improved by timely diagnosis and early treatment[2]. With the aid of imaging, a PE can be more accurately diagnosed on the basis of clinical manifestations that usually exhibit poor specificity[3]. Computed tomography angiography (CTA) is a medical imaging technique that has been widely applied for the diagnosis of vascular diseases due to its advantages of convenience, noninvasiveness, high accuracy, and ability to simultaneously display internal and external vascular lesions[4]. Computed tomography pulmonary angiography (CTPA) is the current gold standard for the diagnosis of suspected acute PE but cannot be offered to patients who have a low glomerular filtration rate[5].

Iodinated contrast media are frequently used injectables that enhance the radiographic visualization of anatomical structures, but the intravascular administration of contrast media is associated with negative outcomes, such as acute kidney injury[6]. Iodinated contrast media can also induce persisting hyperthyroidism or worsen the condition of the disease, particularly in patients with a family history of thyroid diseases[7]. Moreover, intravenous iodinated contrast media increases the risk of acute kidney injury in patients with renal insufficiency or can trigger hypersensitivity reactions[8–10]. The application of iodine-based contrast media may also be complicated for patients with multiple myeloma because they are considered at a very high risk of acute kidney injury[10]. The side effects and limitations of iodinated contrast warrant investigations on an alternative CT contrast medium.

Lanthanide ion gadolinium is the most commonly used metal atom for the enhancement of magnetic

An XIE, E-mail: xiean@hunnu.edu.com; Wen-jie SUN, E-mail: sunwenjie198342@163.com
[†]The authors contributed equally to this research.
[#]Corresponding authors, Feng HUANG, E-mail: huangfeng608@163.com; Jian-bin LIU, E-mail: binban24@hunnu.edu.cn
*This study was supported by grants from the Scientific Research Project of Hunan Health Commission in 2019 (No. B2019071) and the Scientific Research Project of Hunan Health Commission in 2020 (No. B20200059).

resonance imaging (MRI)[11]. Compared with iodinated contrast, a gadolinium-based contrast agent (GBCA) has been shown to reduce the incidence of contrast-induced nephropathy in percutaneous transluminal renal angioplasty[12]. Remy-Jardin *et al* used gadolinium chelates in 16-detector CTPA and yielded favorable diagnostic information[13]. Additionally, the emergence of advanced CT scanners has increased the possibility of using gadolinium-based contrast media. Therefore, this study elucidated the feasibility of using a GBCA [gadopentetate dimeglumine (Gd-DTPA)] for a CTPA in the turbo flash scan mode and also investigated the effect of virtual monoenergetic imaging on contrast enhancement.

1 MATERIALS AND METHODS

1.1 Research Objects

This study involved 66 patients (35 males and 31 females; 20–81 years; 57.7±18.3 years) who underwent a CTPA at Hunan Provincial People's Hospital, China, from February 2019 to October 2019. Inclusion criteria comprised: (1) Patients who needed a CTPA and agreed on using an iohexol injection or Gd-DTPA as a contrast medium, (2) patients who needed enhanced scanning and agreed to add a pulmonary arterial phase scan using iohexol or Gd-DTPA, and (3) ≥18 years. Exclusion criteria consisted of: (1) Severe heart or kidney dysfunction, (2) poor breathing coordination resulting in large breathing artifacts, and (3) pulmonary trunk embolism affecting the measurement of the data. There were nine cases of pleural effusions, six atelectasis, 16 space-occupying lesions of the lung, two pericardial effusions, and two PEs in the selected patients. This study recruited patients who had volunteered to join in this research, and these patients had mild symptoms of a PE or suspected PE. Patients with high pretest risks were excluded because this study was designed to investigate whether gadolinium-enhanced CTA could clearly display the pulmonary arteries and be used for diagnosis of a PE instead of replacing iodine-enhanced CTA. Therefore, the number of positive PE cases was extremely low in the study population, which may not be a good reference for evaluating the diagnostic performance of CTPA.

1.2 Ethics Statement

This study was approved by the Ethics Committee of Hunan Provincial People's Hospital and informed consent from all patients (ethical approval number: 2018-198) was obtained before the experiments. The procedures involving human participants all complied with the Declaration of Helsinki established in June 1964 and subsequent revisions. There was no identifiable patient information in this case report.

1.3 Scanning Methods and Parameters

The SOMATOM Force dual-source CT scanner (Siemens, Germany) was used in this study. The patient underwent respiratory training before a CT scan was performed during the maximum end-inspiratory pause. The patient lied supine and was scanned feet first and from the tip to the bottom of the lung. A dual-cylinder syringe was used to inject iohexol (350 mg/mL) or Gd-DTPA (469.01 mg/mL) at a dose of 0.6 mL/kg into the left elbow vein at a rate of 5 mL/s. After injecting with the contrast agent, the patient was additionally injected with 30 mL of normal saline. The region of interest (ROI) was set in the horizontal pulmonary artery trunk below the tracheal bifurcation, and the scan was triggered when the CT value increased by 50 Hu on the basis of the plain scan. The CT images were reconstructed using a 1.0 mm slice thickness and 1.0 mm slice interval. The 66 patients were randomly divided into three groups (Group A, B, and C; 22 patients per group). Group A underwent turbo flash scanning using an iohexol injection (100 kVp tube voltage, automatic tube current, 2.8 mm pitch, 0.6 mm collimation width, and 0.25 s/cycle speed). Group B underwent turbo flash scanning using Gd-DTPA (70 kVp tube voltage, automatic tube current, 2.8 mm pitch, 0.6 mm collimation width, and 0.25 s/cycle speed). Group C underwent dual-energy scanning using Gd-DTPA (70/Sn150 kVp tube voltage, automatic tube current, 1.2 mm pitch, 0.6 mm collimation width, and 0.5 s/cycle speed).

1.4 Image Processing

The original images were imported into the Siemens post-processing workstation (syngo.via). The "CT angiography" software window was run to obtain virtual reality (VR) and maximum intensity projection (MIP) images, and a high-resolution soft tissue window (600 Hu width; 150 Hu level) was reconstructed. The dual-energy scanning data obtained at 70 kVp represented the data of Group C (70 kVp; Sn150 kVp). The images of Group C were run in the "dual energy" software window under the mono+mode (virtual monoenergetic imaging) to obtain axial images at 40, 50, 60, 70, 80, 90, 100, and 110 keV, respectively (1.0 mm slice thickness, 1.0 mm slice interval, 600 Hu window width, and 150 Hu window level). The images of Group C were also reconstructed as linear-blended images by applying a blending factor of 0.5 at the workstation.

1.5 Measurement and Evaluation of the Pulmonary Artery CT Values

The CT values of the pulmonary artery trunk, left pulmonary artery, and right pulmonary artery were measured at the pulmonary artery bifurcation level simultaneously, thus avoiding the beam hardening artifacts of the superior vena cava (SVC). The area of the ROI was 0.5 cm^2.

1.6 Image Quality Evaluation

The signal-to-noise ratio (SNR) and contrast-to-noise ratio (CNR) were calculated according to the following formulas: SNR=the CT value of the pulmonary artery trunk/the standard deviation of the right paraspinal muscle CT value; CNR=(the CT value of the pulmonary artery trunk – the CT value of the right paraspinal muscle)/the standard deviation of the right paraspinal muscle CT value.

Two radiologists with three and 11 years of imaging diagnosis experience, respectively, independently evaluated whether there were beam hardening artifacts of the SVC. A consensus on the evaluations was reached if there were differences.

The two radiologists independently determined the vascular branching series based on the VR, MIP, and high-resolution soft tissue window images. A unanimous result was obtained if the two grades obtained were inconsistent. Vascular branching series had 6 grades: grade 1, pulmonary artery trunk; grade 2, right pulmonary artery; grade 3, right interlobular artery; grade 4, right lower lobe artery; grade 5, right lower lobe segmental artery; grade 6, right lower lobe segmental arterial branches.

The two radiologists scored the overall image quality by using a five-point Likert scale[14]. The scale was as follows: 1 point, images with poor quality that could not be used for diagnosis; 2 points, suboptimal enhancement and noise interference with diagnostic confidence; 3 points, acceptable enhancement and moderate noise without affecting the diagnostic confidence; 4 points, typical enhancement and noise for the evaluation of the vascular and extravascular structures; and 5 points, homogeneous enhancement and minimal noise, which was optimal for vascular evaluation.

1.7 Radiation Dose

The volume CT dose index (CTDI vol) and dose length product (DLP) were calculated based on the CT-dose table.

1.8 Statistical Analysis

SPSS 21.0 software (SPSS Inc, USA) was used for the statistical analysis. Measurement data, such as age, body mass index (BMI), and CT value were expressed as the mean±standard deviation (SD), while enumeration data, such as pleural effusion, atelectasis, space-occupying, pericardial effusion, vascular branching series, and hardening artifacts were expressed as percentages. The *t*-test (for the two groups) and analysis of variance (for the multiple groups) were used to compare the measurement data. The least significance difference test or Tukey's test was used for post hoc multiple comparisons. The enumeration data were compared using the *Chi*-squared test. Differences were considered statistically significant at $P<0.05$.

2 RESULTS

2.1 Basic Information and Clinical Characteristics of the Patients

A total of 66 patients were enrolled in this study, including 35 males and 31 females. The average age, gender, BMI and clinical characteristics of Groups A, B and C (n=22 per group) are listed in table 1 and showed no significant difference ($P>0.05$).

2.2 Pulmonary Artery CT Values

The CT values of the pulmonary artery trunk, left pulmonary artery, and right pulmonary artery of Group A were significantly higher than those of Groups B and C (table 2; $P<0.001$). Group A used an iodinated contrast agent, while Groups B and C used Gd-DTPA. The concentration of gadolinium was lower than that of iodine. Therefore, the CT values of Groups B and C were not as high as that of Group A. There were no significant differences in the pulmonary artery CT values between Groups B and C (table 2; $P>0.05$). The CT values of the pulmonary artery trunk, left pulmonary artery, and right pulmonary artery all met the diagnostic standards.

2.3 Image Quality Evaluation

The SNR and CNR in Group A were significantly higher than those in Groups B and C (table 3, $P<0.0001$). There was no significant differences in either the SNR or CNR between Groups B and C (P=0.587; P=0.259). The proportions of beam hardening artifacts of the SVC in Groups A, B, and C were 90.9%, 22.7%, and 13.6%, respectively and showed statistically significant differences (table

Table 1 Basic information and clinical characteristics of patients [*n* (%), mean±SD]

Parameters	Group A	Group B	Group C	F/χ^2	*P*
Age (years)	62.4±11.3	60.7±12.5	58.7±14.2	0.466	0.629
Gender					
Male	12 (54.5)	9 (40.9)	14 (63.6)	2.312	0.315
BMI (kg/m^2)	23.3±4.5	21.6±3.1	22.6±3.8	1.088	0.343
Clinical characteristics					
Pleural effusion	2 (9.1)	4 (18.2)	3 (13.6)	0.772	0.679
Atelectasis	2 (9.1)	1 (4.5)	3 (13.6)	1.100	0.576
Space-occupying	7 (31.8)	5 (22.7)	4 (18.2)	1.113	0.573
Pericardial effusion	1 (4.5)	0 (0)	1 (4.5)	1.031	0.597
Pulmonary embolism	1 (4.5)	0 (0)	1 (4.5)	1.031	0.597

Table 2 Pulmonary artery CT values (mean±SD)

	Group A	Group B	Group C	F	*P*
Pulmonary artery trunk (Hu)	552.66±92.54	262.34±64.87	256.19±48.45	125.3	<0.0001
Left pulmonary artery (Hu)	483.62±103.28	258.78±53.64	249.74±53.62	70.57	<0.0001
Right pulmonary artery (Hu)	498.4±101.38	248.15±58.49	246.85±56.29	382.11	<0.0001

Table 3 Image quality evaluation [*n* (%), mean±SD]

	Group A	Group B	Group C	Z/χ^2	*P*
Vascular branching series					
Grade 5	19 (86.4)	11 (50.0)	13 (59.1)	6.94	0.0311
Grade 6	3 (13.6)	11 (50.0)	9 (40.9)		
Beam hardening artifacts	20 (90.9)	5 (22.7)	3 (13.6)	29.65	<0.0001
Subjective scores					
3	0 (0)	1 (4.6)	0 (0)		
4	4 (18.2)	9 (40.9)	7 (31.8)	5.1	0.2772
5	18 (81.8)	12 (54.5)	15 (68.2)		
SNR	49.53±15.47	21.58±8.49	18.44±4.68	58.01	<0.0001
CNR	45.28±13.27	17.59±8.16	13.02±5.61	73.36	<0.0001

SNR: signal-to-noise ratio; CNR: contrast-to-noise ratio

3; *P*<0.0001). The vascular branching series of the three groups also had significant differences (table 3; *P*=0.0311). The pairwise comparisons showed that the vascular branching series of Groups B and C were significantly superior to those of Group A (*P*=0.0096; *P*=0.0423), but there was no significant difference between Groups B and C (*P*=0.5448). Furthermore, there were no significant differences in the subjective scores of the three groups (table 3; fig. 1A–1C).

2.4 Radiation Doses

The CTDI vol and DLP of Groups A, B and C showed significant differences (table 4; *P*<0.0001, CTDI vol/$DLP_{group\ C}$>CTDI vol/$DLP_{group\ A}$>CTDI vol/$DLP_{group\ B}$). In the pairwise comparisons, the differences between the groups were also statistically significant (CTDI vol: *P*=0.0116, *P*=0.0003, and *P*<0.0001; DLP: *P*=0.0027, *P*<0.0001, and *P*<0.0001).

2.5 Evaluations of the Reconstructed Images of Group C

The CT values of the pulmonary artery trunk, left pulmonary artery, and right pulmonary artery of Group $C_{40\ keV}$ were significantly higher than those of the other post-processing groups. The pulmonary artery CT values of all the post-processing groups are listed in table 5.

There was significant difference in the image quality of these post-processing groups (table 6). The SNR (19.85±6.82), CNR (15.13±5.84), vascular branching series (grade 6; 81.8%) and subjective score (5 points; 95.4%) of Group $C_{40\ keV}$ were the highest among these post-processing groups. The beam

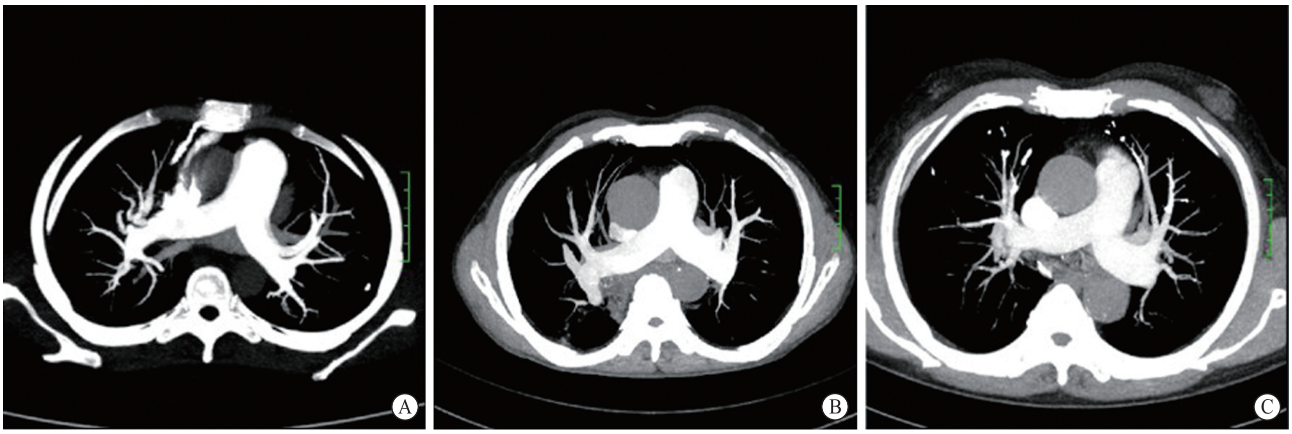

Fig. 1 VR images of the pulmonary arteries

A: high-pitch helical scanning using an iohexol injection; B: High-pitch helical scanning using gadopentetate dimeglumine; C: dual-energy scanning using gadopentetate dimeglumine. These three images all had grade 6 vascular branching series and scored five points (excellent) in the subjective evaluation.

Table 4 Radiation doses (mean±SD)

	Group A	Group B	Group C	F	*P*
CTDI vol (mGy)	3.65±1.42	2.25±0.8	4.39±0.93	25.86	<0.0001
DLP (mGy•cm)	102.45±52.82	58.88±26.48	159.28±41.26	32.21	<0.0001

CTDI vol: the volume CT dose index; DLP: dose length product

Table 5 Pulmonary artery CT values of post-processing groups (mean±SD)

	Pulmonary artery trunk (Hu)	Left pulmonary artery (Hu)	Right pulmonary artery (Hu)
$C_{m0.5}$	173.52±46.28	168.28±43.06	171.20±37.59
$C_{40\ keV}$	371.42±76.28	361.51±82.50	372.62±82.16
$C_{50\ keV}$	284.22±56.29	278.45±61.22	269.28±65.18
$C_{60\ keV}$	216.45±52.28	213.61±43.29	208.19±53.49
$C_{70\ keV}$	176.42±46.79	165.29±46.24	171.26±42.39
$C_{80\ keV}$	151.26±35.85	146.51±43.28	142.45±26.22
$C_{90\ keV}$	135.51±33.35	127.58±226.52	130.28±30.59
$C_{100\ keV}$	126.34±30.26	117.49±30.22	126.12±25.81
$C_{110\ keV}$	109.28±16.94	102.28±17.49	106.3±20.18
P	<0.0001	<0.0001	<0.0001

hardening artifact ratio of Group $C_{40\ keV}$ was 18.2%, which was only below that of Group $C_{50\ keV}$. In the pairwise comparisons, the SNR, CNR, beam hardening artifact ratio, vascular branching series, and subjective score of Group $C_{40\ keV}$ were significantly different from those of Groups $C_{80\ keV}$, $C_{90\ keV}$, $C_{100\ keV}$, and $C_{110\ keV}$, but not Groups $C_{m0.5}$, $C_{50\ keV}$, $C_{60\ keV}$, and $C_{70\ keV}$.

2.6 Comparisons of Group $C_{40\ keV}$ to Groups A, B, and C

The CT values of the pulmonary artery trunk, left pulmonary artery, and right pulmonary artery of Group $C_{40\ keV}$ were significantly higher than those of Groups B and C, but lower than those of Group A (table 7; all *P*<0.0001).

Table 6 Image quality of post-processing groups [*n* (%), mean±SD]

	$C_{m0.5}$	$C_{40\ keV}$	$C_{50\ keV}$	$C_{60\ keV}$	$C_{70\ keV}$	$C_{80\ keV}$	$C_{90\ keV}$	$C_{100\ keV}$	$C_{110\ keV}$	*P*
Vascular branching										
Grade 3	0	0	0	0	0	0	2 (9.1)	5 (22.7)	8 (36.4)	<0.0001
Grade 4	2 (9.0)	0	0	0	2 (9.1)	4 (18.2)	10 (45.5)	12 (54.6)	11 (50.0)	
Grade 5	10 (45.5)	4 (18.2)	5 (22.7)	5 (22.7)	8 (36.4)	15 (68.2)	9 (40.9)	5 (22.7)	3 (13.6)	
Grade 6	10 (45.5)	18 (81.8)	17 (77.3)	17 (77.3)	12 (54.5)	3 (13.6)	1 (4.5)	0	0	
Beam hardening	2 (9.1)	4 (18.2)	7 (31.8)	3 (14.3)	2 (13.6)	1 (4.5)	0	0	0	0.1344
Subjective score										
2 points	0	0	0	0	0	0	0	2 (9.1)	4 (18.1)	<0.0001
3 points	1 (4.5)	0	0	0	1 (4.5)	2 (9.0)	4 (18.2)	5 (22.7)	8 (36.4)	
4 points	8 (36.4)	1 (4.5)	2 (9.0)	4 (18.2)	5 (22.7)	10 (45.5)	11 (50.0)	13 (59.1)	10 (45.5)	
5 points	13 (59.1)	21 (95.4)	20 (91.0)	18 (81.2)	16 (72.8)	10 (45.5)	7 (31.8)	2 (9.1)	0	
SNR	16.43±4.12	19.85±6.82	18.45±6.35	17.13±4.25	16.85±6.23	15.94±5.22	15.34±4.55	14.51±4.53	13.84±4.16	<0.0001
CNR	11.35±3.26	15.13±5.84	14.03±5.28	11.3±4.82	10.26±5.16	9.81±4.16	9.32±3.26	8.48±3.58	7.86±43.58	<0.0001

Note: Figures in the parentheses are percentages.

Table 7 Pulmonary artery CT values of group A, B, C and $C_{40\ keV}$

	Pulmonary artery trunk (Hu)	Left pulmonary artery (Hu)	Right pulmonary artery (Hu)
Group A	552.66±92.54	483.62±103.28	498.4±101.38
Group B	262.34±64.87	258.78±53.64	248.15±58.49
Group C	256.19±48.45	249.74±53.62	246.85±56.29
Group $C_{40\ keV}$	371.42±76.28	361.51±82.50	372.62±82.16
P (A *vs.* $C_{40\ keV}$)	<0.0001	<0.0001	<0.0001
P (B *vs.* $C_{40\ keV}$)	<0.0001	<0.0001	<0.0001
P (C *vs.* $C_{40\ keV}$)	<0.0001	<0.0001	<0.0001

The vascular branching series of Group $C_{40\ keV}$ were much higher than those of Group A (table 8; *P*<0.0001). The SNR, CNR, and beam hardening artifact ratio of Group $C_{40\ keV}$ were significantly lower than those of Group A (table 8; *P*<0.0001). Group $C_{40\ keV}$ also had higher subjective scores than Group A (table 8, *P*=0.1541). Compared with Group B, Group $C_{40\ keV}$ showed a superior vascular branching series and subjective scores (table 8; *P*=0.0260 and *P*=0.019). Group $C_{40\ keV}$ also had a higher vascular branching series than Group C (table 8; *P*=0.0053), but showed no significant differences from Group C in the subjective scores. There were no significant differences in the SNR, CNR, and beam hardening artifacts between Groups $C_{40\ keV}$ and B or between Groups $C_{40\ keV}$ and C.

3 DISCUSSION

Dual-energy CT, also known as spectral CT, is a technique that uses two separate energy spectra to obtain images similar to those generated by traditional single-energy CT. Currently, there are six types of dual-energy CT scanners: single-source helical dual-energy CT (Siemens Healthineers, Germany), single-

Table 8 Image quality of group A, B, C and $C_{40\ keV}$ [*n* (%), mean±SD]

	Group A	Group B	Group C	Group $C_{40\ keV}$	*P* (A *vs*. $C_{40\ keV}$)	*P* (B *vs*. $C_{40\ keV}$)	*P* (C *vs*. $C_{40\ keV}$)
Vascular branching series							
Grade 5	19 (86.4)	11 (50.0)	13 (59.1)	4 (18.2)	<0.0001	0.026	0.0053
Grade 6	3 (13.6)	11 (50.0)	9 (40.9)	18 (81.8)			
Beam hardening artifacts	20 (90.9)	5 (22.7)	3 (13.6)	4 (18.2)	<0.0001	0.7086	0.6802
Subjective score							
3 points	0 (0)	1 (4.6)	0 (0)	0 (0)			
4 points	4 (18.2)	9 (40.9)	7 (31.8)	1 (4.5)	0.1541	0.019	0.4531
5 points	18 (81.8)	12 (54.5)	15 (68.2)	21 (95.4)			
SNR	49.53 ± 15.47	21.58 ± 8.49	18.44 ± 4.68	19.85 ± 6.82	<0.0001	0.9352	0.9633
CNR	45.28 ± 13.27	17.59 ± 8.16	13.02 ± 5.61	15.13 ± 5.84	<0.0001	0.7892	0.8555

Note: Figures in the parentheses are percentages. SNR: signal-to-noise ratio; CNR: contrast-to-noise ratio

source sequential dual-energy CT (Toshiba, Japan), single-source fast kVp switching dual-energy CT (GE Healthcare, USA), single-source twin-beam dual-energy CT (Siemens Healthineers), dual-source dual-energy CT (Siemens Healthineers), and dual-layer dual-energy CT (Philips Healthcare, Best, the Netherlands)[15]. This study used SOMATOM Force dual-source CT, one type of dual-energy CT, which provided four tube voltages for dual-energy scanning: 70/150 SnkVp, 80/150 SnkVp, 90/150 SnkVp, and 100/150 SnkVp, respectively[16]. Turbo flash scan is a unique scanning mode of dual-source CT, which is equipped with two X-ray tube/detector systems and presents the advantages, such as fast scanning speed and low radiation dosage[17, 18]. This study compared the differences in image quality and contrast enhancement between dual-energy scanning (70/150 SnkVp) and turbo flash scanning when Gd-DTPA was used as a contrast agent.

The current concentration of gadolinium in commercial contrast agents for clinical use is only 0.5 mmol/mL, which is significantly lower than that of iodine (2.4 mmol/mL) in a 300 mgI/mL contrast agent. Therefore, when a contrast agent was injected at the same speed and same dose, the intravascular concentration of gadolinium was about one-fifth of that of iodine, which limited the use of gadolinium for the CTA enhancement. Additionally, the general maximum dose of a gadolinium contrast agent was 0.3 mmol/kg[19]. In this case, 40 mL of 0.5 mmol/mL Gd-DTPA was used in an adult weighing 70 kg, which was equivalent to about 8 mL of an iodinated contrast agent of the same mmol concentration. Nonetheless, there was evidence supporting the feasibility of a gadolinium-enhanced CTA[20, 21]. MRI with Gd-DTPA was proven to be a safe imaging modality in liver transplanted patients, and this intravenous contrast medium was suggested for contrast-enhanced CT in patients with renal insufficiency[22]. High-quality CTPA images could be produced with low-dose contrast media[23, 24], which also increased the possibility of using gadolinium-based contrast media for a CTPA.

Despite the potential for CTA contrast, gadolinium-based contrast agents were also associated with adverse side effects (0.01%–2% occurrence rate) in MRI[25–32]. The most common side effects of gadolinium-based contrast agents were urticaria-like reactions, and the incidence of life-threatening allergic reactions ranges between 0.001% and 0.01%[33–35]. Overall, the incidence of gadolinium-related adverse events was far lower than that of iodine-related adverse events[35]. In the past two decades, studies on the safety of gadolinium contrast agents have focused on nephrogenic systemic fibrosis and gadolinium deposition[36]. Gadolinium can be deposited in human tissues, such as the brain, bones, and liver[37–40]. McDonald *et al* reported that gadolinium was deposited in a dose-dependent manner in neural tissues of patients after intravenous injection of a gadolinium-based contrast agent in the absence of intracranial abnormalities or renal dysfunction[39, 41]. The form of the deposited gadolinium (chelated or non-chelated) and the pathophysiology of this deposition were not fully understood[42]. Kanda *et al* believed that free gadolinium ions were replaced by other endogenous metal ions in the body, such as iron, copper, and zinc[43]. Another theory proposed that gadolinium was transported across the blood-brain barrier by specific metal transporters[44]. However, so far, there has been no irrefutable evidence showing the clinical side effects of the gadolinium deposition[39, 45, 46]. Fortunately, there was no gadolinium deposition in the brain seen in this study, but the neurotoxic mechanism of the deposited gadolinium and how it could be cleared would need further exploration for safer use of a gadolinium-based contrast agent.

The safe dose of a gadolinium-based contrast agent in human was 0.3–0.5 mmol/kg[47]. Correspondingly, the safe dose of Gd-DTPA (469.01 mg/mL) was 0.6–1.0 mL/kg. For safety reasons, the dose of Gd-DTPA used in this study was 0.6 mL/kg. Moreover, the bolus tracking technique instead of test bolus was applied to reduce the usage of Gd-DTPA, and the triggering threshold was 50 Hu (i.e., the scan was triggered when the CT value was increased by 50 Hu on the basis of a plain scan). Becker *et al* believed that a CT value of 250–350 Hu indicated qualified diagnostic images of intravascular structures[48]. From the data in table 2, when Gd-DTPA was used as a contrast agent for a CTPA, both the turbo flash scanning (Group B) and dual-energy scanning (Group C) generated images with diagnostic significance. There were no significant differences in the pulmonary artery CT values, subjective scores of image quality, the SNR, and CNR between these two groups. However, Group B had a significantly lower CTDI vol and DLP than Group C. Compared with turbo flash scanning (2.8 mm pitch), dual-energy scanning (1.2 mm pitch) required a longer scan time and used two X-ray tubes, which resulted in the higher radiation dose. Therefore, a turbo flash scan was recommended as the first choice for emergency CTPA since it not only generated qualified images, but also reduced the examination duration and radiation dose. In addition, motion artifacts could be reduced by shortening the scan duration, which was associated with a clearer display of the blood vessels[49].

Virtual monoenergetic images (VMIs), such as virtual non-contrast and calcium subtraction images, could be produced from linear or non-linear blending of dual-energy CT images[50, 51]. From previous studies, the best quality of the VMIs could be achieved when the images were generated at 40–50 keV or reconstructed as linear-blended images by applying a blending factor of 0.5[52, 53]. In this study, the images of Group C were reconstructed at 40, 50, 60, 70, 80, 90, 100, and 110 keV, respectively, or linearly blended with a blending factor of 0.5 (M_0.5; 50% of the low-kV and 50% of the high-kV spectrum). Group $C_{40\ keV}$ showed the highest pulmonary artery CT values and the best displaying of vascular branches compared with the other energy groups and Group B. Reconstruction of the linear-blended images by applying a blending factor of 0.5 did not increase the contrast enhancement.

This study proved the feasibility of using Gd-DTPA for CTPA. The dual-energy and turbo flash scanning modes showed no significant differences in image quality. Compared with dual-energy scanning, turbo flash scanning reduced the scan duration and radiation dose. Virtual monoenergetic imaging at 40 keV further improved the contrast of the target vessels and enhanced the displaying of the peripheral vessels, thus adding to the diagnostic confidence of gadolinium-enhanced CTPA. Theoretically, the protocols adopted by this research could work on all the other spiral CT scanners which are able to perform pulmonary CTA. Finally, further research could be done to compare the image quality between dual-energy and other gadolinium-based CTPA.

Conflict of Interest Statement

The authors declare that there is no conflict of interest with any financial organization or corporation or individual that can inappropriately influence this work.

REFERENCES

1 Essien EO, Rali P, Mathai SC. Pulmonary Embolism. Med Clin North Am, 2019,103(3):549-564
2 Mansella G, Keil C, Nickel CH, *et al*. Delayed Diagnosis in Pulmonary Embolism: Frequency, Patient Characteristics, and Outcome. Respiration, 2020,99(7):589-597
3 Di Nisio M, van Es N, Buller HR. Deep vein thrombosis and pulmonary embolism. Lancet, 2016,388(10063):3060-3073
4 Grabherr S, Heinemann A, Vogel H, *et al*. Postmortem CT Angiography Compared with Autopsy: A Forensic Multicenter Study. Radiology, 2018,288(1):270-276
5 Moore AJE, Wachsmann J, Chamarthy MR, *et al*. Imaging of acute pulmonary embolism: an update. Cardiovasc Diagn Ther, 2018,8(3):225-243
6 Lakhal K, Ehrmann S, Robert-Edan V. Iodinated contrast medium: Is there a re(n)al problem? A clinical vignette-based review. Crit Care, 2020,24(1):641
7 Bonelli N, Rossetto R, Castagno D, *et al*. Hyperthyroidism in patients with ischaemic heart disease after iodine load induced by coronary angiography: Long-term follow-up and influence of baseline thyroid functional status. Clin Endocrinol (Oxf), 2018,88(2):272-278
8 Davenport MS, Perazella MA, Yee J, *et al*. Use of Intravenous Iodinated Contrast Media in Patients with Kidney Disease: Consensus Statements from the American College of Radiology and the National Kidney Foundation. Radiology, 2020,294(3):660-668
9 Dona I, Bogas G, Salas M, *et al*. Hypersensitivity Reactions to Multiple Iodinated Contrast Media. Front Pharmacol, 2020,11:575437
10 Stacul F, Bertolotto M, Thomsen HS, *et al*. Iodine-based contrast media, multiple myeloma and monoclonal gammopathies: literature review and ESUR Contrast Media Safety Committee guidelines. Eur Radiol, 2018,28(2):683-691
11 Xiao YD, Paudel R, Liu J, *et al*. MRI contrast agents: Classification and application (Review). Int J Mol Med, 2016,38(5):1319-1326
12 Kane GC, Stanson AW, Kalnicka D, *et al*. Comparison between gadolinium and iodine contrast for percutaneous intervention in atherosclerotic renal artery stenosis: clinical outcomes. Nephrol Dial Transplant, 2008,23(4):1233-1240
13 Remy-Jardin M, Bahepar J, Lafitte JJ, *et al*. Multi-detector row CT angiography of pulmonary circulation with gadolinium-based contrast agents: prospective evaluation in 60 patients. Radiology, 2006,238(3):1022-1035
14 Patino M, Parakh A, Lo GC, *et al*. Virtual Monochromatic Dual-Energy Aortoiliac CT Angiography With Reduced Iodine Dose: A Prospective Randomized Study. AJR Am J Roentgenol, 2019,212(2):467-474
15 De Santis D, Eid M, De Cecco CN, *et al*. Dual-Energy Computed Tomography in Cardiothoracic Vascular Imaging. Radiol Clin North Am, 2018,56(4):521-534
16 Siegel MJ, Kaza RK, Bolus DN, *et al*. White Paper of the Society of Computed Body Tomography and Magnetic

Resonance on Dual-Energy CT, Part 1: Technology and Terminology. J Comput Assist Tomogr, 2016,40(6):841-845
17 Deseive S, Pugliese F, Meave A, *et al*. Image quality and radiation dose of a prospectively electrocardiography-triggered high-pitch data acquisition strategy for coronary CT angiography: The multicenter, randomized PROTECTION IV study. J Cardiovasc Comput Tomogr, 2015,9(4):278-285
18 Flohr TG, Leng S, Yu L, *et al*. Dual-source spiral CT with pitch up to 3.2 and 75 ms temporal resolution: image reconstruction and assessment of image quality. Med Phys, 2009,36(12):5641-5653
19 Thurnher SA, Capelastegui A, Del Olmo FH, *et al*. Safety and effectiveness of single- versus triple-dose gadodiamide injection-enhanced MR angiography of the abdomen: a phase III double-blind multicenter study. Radiology, 2001,219(1):137-146
20 Chicoskie C, Tello R. Gadolinium-enhanced MDCT angiography of the abdomen: feasibility and limitations. AJR Am J Roentgenol, 2005,184(6):1821-1828
21 Nadjiri J, Pfeiffer D, Straeter AS, *et al*. Spectral Computed Tomography Angiography With a Gadolinium-based Contrast Agent: First Clinical Imaging Results in Cardiovascular Applications. J Thorac Imaging, 2018,33(4):246-253
22 Flynn MM, Parekh AN, Parikh MR, *et al*. Renal Safety of Intravenous Gadolinium-enhanced MRI in Patients Following Liver Transplantation. Transplantation, 2019,103(6):e159-e163
23 Rajiah P, Ciancibello L, Novak R, *et al*. Ultra-low dose contrast CT pulmonary angiography in oncology patients using a high-pitch helical dual-source technology. Diagn Interv Radiol, 2019,25(3):195-203
24 Silva M, Milanese G, Cobelli R, *et al*. CT angiography for pulmonary embolism in the emergency department: investigation of a protocol by 20 ml of high-concentration contrast medium. Radiol Med, 2020,125(2):137-144
25 Abujudeh HH, Kosaraju VK, Kaewlai R. Acute adverse reactions to gadopentetate dimeglumine and gadobenate dimeglumine: experience with 32,659 injections. AJR Am J Roentgenol, 2010,194(2):430-434
26 Aran S, Shaqdan KW, Abujudeh HH. Adverse allergic reactions to linear ionic gadolinium-based contrast agents: experience with 194, 400 injections. Clin Radiol, 2015,70(5):466-475
27 Bleicher AG, Kanal E. Assessment of adverse reaction rates to a newly approved MRI contrast agent: review of 23,553 administrations of gadobenate dimeglumine. AJR Am J Roentgenol, 2008,191(6):W307-311
28 Bruder O, Schneider S, Pilz G, *et al*. 2015 Update on Acute Adverse Reactions to Gadolinium based Contrast Agents in Cardiovascular MR. Large Multi-National and Multi-Ethnical Population Experience With 37788 Patients From the EuroCMR Registry. J Cardiovasc Magn Reson, 2015,17(1):58
29 Hunt CH, Hartman RP, Hesley GK. Frequency and severity of adverse effects of iodinated and gadolinium contrast materials: retrospective review of 456,930 doses. AJR Am J Roentgenol, 2009,193(4):1124-1127
30 Matsumura T, Hayakawa M, Shimada F, *et al*. Safety of gadopentetate dimeglumine after 120 million administrations over 25 years of clinical use. Magn Reson Med Sci, 2013,12(4):297-304
31 Uhlig J, Lucke C, Vliegenthart R, *et al*. Acute adverse events in cardiac MR imaging with gadolinium-based contrast agents: results from the European Society of Cardiovascular Radiology (ESCR) MRCT Registry in 72,839 patients. Eur Radiol, 2019,29(7):3686-3695
32 Young LK, Matthew SZ, Houston JG. Absence of potential gadolinium toxicity symptoms following 22,897 gadoteric acid (Dotarem(R)) examinations, including 3,209 performed on renally insufficient individuals. Eur Radiol, 2019,29(4):1922-1930
33 Haneder S, Kucharczyk W, Schoenberg SO, *et al*. Safety of magnetic resonance contrast media: a review with special focus on nephrogenic systemic fibrosis. Top Magn Reson Imaging, 2015,24(1):57-65
34 Murphy KJ, Brunberg JA, Cohan RH. Adverse reactions to gadolinium contrast media: a review of 36 cases. AJR Am J Roentgenol, 1996,167(4):847-849
35 Runge VM. Safety of approved MR contrast media for intravenous injection. J Magn Reson Imaging, 2000,12(2):205-213
36 Woolen SA, Shankar PR, Gagnier JJ, *et al*. Risk of Nephrogenic Systemic Fibrosis in Patients With Stage 4 or 5 Chronic Kidney Disease Receiving a Group Ⅱ Gadolinium-Based Contrast Agent: A Systematic Review and Meta-analysis. JAMA Intern Med, 2020,180(2):223-230
37 Kanda T, Fukusato T, Matsuda M, *et al*. Gadolinium-based Contrast Agent Accumulates in the Brain Even in Subjects without Severe Renal Dysfunction: Evaluation of Autopsy Brain Specimens with Inductively Coupled Plasma Mass Spectroscopy. Radiology, 2015,276(1):228-232
38 Maximova N, Gregori M, Zennaro F, *et al*. Hepatic Gadolinium Deposition and Reversibility after Contrast Agent-enhanced MR Imaging of Pediatric Hematopoietic Stem Cell Transplant Recipients. Radiology, 2016,281(2):418-426
39 McDonald RJ, McDonald JS, Kallmes DF, *et al*. Gadolinium Deposition in Human Brain Tissues after Contrast-enhanced MR Imaging in Adult Patients without Intracranial Abnormalities. Radiology, 2017,285(2):546-554
40 Murata N, Gonzalez-Cuyar LF, Murata K, *et al*. Macrocyclic and Other Non-Group 1 Gadolinium Contrast Agents Deposit Low Levels of Gadolinium in Brain and Bone Tissue: Preliminary Results From 9 Patients With Normal Renal Function. Invest Radiol, 2016,51(7):447-453
41 McDonald RJ, McDonald JS, Kallmes DF, *et al*. Intracranial Gadolinium Deposition after Contrast-enhanced MR Imaging. Radiology, 2015,275(3):772-782
42 Layne KA, Dargan PI, Archer JRH, *et al*. Gadolinium deposition and the potential for toxicological sequelae - A literature review of issues surrounding gadolinium-based contrast agents. Br J Clin Pharmacol, 2018,84(11):2522-2534
43 Kanda T, Nakai Y, Oba H, *et al*. Gadolinium deposition in the brain. Magn Reson Imaging, 2016,34(10):1346-1350

44 Iliff JJ, Wang M, Liao Y, *et al*. A paravascular pathway facilitates CSF flow through the brain parenchyma and the clearance of interstitial solutes, including amyloid beta. Sci Transl Med, 2012,4(147):147ra111

45 Malikova H. Nephrogenic systemic fibrosis: the end of the story? Quant Imaging Med Surg, 2019,9(8):1470-1474

46 Taoka T, Naganawa S. Gadolinium-based Contrast Media, Cerebrospinal Fluid and the Glymphatic System: Possible Mechanisms for the Deposition of Gadolinium in the Brain. Magn Reson Med Sci, 2018,17(2):111-119

47 Esteban JM, Alonso A, Cervera V, *et al*. One-molar gadolinium chelate (gadobutrol) as a contrast agent for CT angiography of the thoracic and abdominal aorta. Eur Radiol, 2007,17(9):2394-2400

48 Becker CR, Hong C, Knez A, *et al*. Optimal contrast application for cardiac 4-detector-row computed tomography. Invest Radiol, 2003,38(11):690-694

49 Kalisz K, Buethe J, Saboo SS, *et al*. Artifacts at Cardiac CT: Physics and Solutions. Radiographics, 2016,36(7):2064-2083

50 Holmes DR, 3rd, Fletcher JG, Apel A, *et al*. Evaluation of non-linear blending in dual-energy computed tomography. Eur J Radiol, 2008,68(3):409-413

51 Silva AC, Morse BG, Hara AK, *et al*. Dual-energy (spectral) CT: applications in abdominal imaging. Radiographics, 2011,31(4):1031-1046, discussion 1047-1050

52 Behrendt FF, Schmidt B, Plumhans C, *et al*. Image fusion in dual energy computed tomography: effect on contrast enhancement, signal-to-noise ratio and image quality in computed tomography angiography. Invest Radiol, 2009,44(1):1-6

53 Grant KL, Flohr TG, Krauss B, *et al*. Assessment of an advanced image-based technique to calculate virtual monoenergetic computed tomographic images from a dual-energy examination to improve contrast-to-noise ratio in examinations using iodinated contrast media. Invest Radiol, 2014,49(9):586-592

(Received Jul. 19, 2021; accepted Jan. 6, 2022)